



Published in final edited form as:

*Biomol NMR Assign.* 2018 April ; 12(1): 183–187. doi:10.1007/s12104-018-9806-7.

## NMR resonance assignments of RNase P protein from *Thermotoga maritima*

Danyun Zeng<sup>1</sup>, Benjamin P Brown<sup>2</sup>, Markus W. Voehler<sup>3</sup>, Sheng Cai<sup>1</sup>, and Nicholas J. Reiter<sup>1,\*</sup>

<sup>1</sup>Department of Chemistry, Marquette University, Milwaukee, Wisconsin, United States of America

<sup>2</sup>Chemical and Physical Biology Program, Vanderbilt University, Nashville, Tennessee, United States of America

<sup>3</sup>Center for Structural Biology Vanderbilt University, Nashville, Tennessee, United States of America

### Abstract

Ribonuclease P (RNase P) is an essential metallo-endonuclease that catalyzes 5' precursor-tRNA (ptRNA) processing and exists as an RNA-based enzyme in bacteria, archaea, and eukaryotes. In bacteria, a large catalytic RNA and a small protein component assemble to recognize and accurately cleave ptRNA and tRNA-like molecular scaffolds. Substrate recognition of ptRNA by bacterial RNase P requires RNA-RNA shape complementarity, intermolecular base pairing, and a dynamic protein-ptRNA binding interface. To gain insight into the binding specificity and dynamics of the bacterial protein-ptRNA interface, we report the backbone and side chain <sup>1</sup>H, <sup>13</sup>C, and <sup>15</sup>N resonance assignments of the hyperthermophilic *Thermotoga maritima* RNase P protein in solution at 318 K. Our data confirm the formation of a stable RNA recognition motif (RRM) with intrinsic heterogeneity at both the N- and C-terminus of the protein, consistent with available structural information. Comprehensive resonance assignments of the bacterial RNase P protein serve as an important first step in understanding how coupled RNA binding and protein-RNA conformational changes give rise to ribonucleoprotein function.

### Keywords

NMR resonance assignment; *Thermotoga maritima*; RNase P; protein-tRNA binding; ribonucleoprotein; TALOS-N prediction

### Biological Context

Ribonucleoprotein complexes (RNPs) assemble into defined tertiary architectures and undergo dynamic interactions to catalyze and mediate fundamental cellular reactions. Ribonuclease P (RNase P) is an essential ribonucleoprotein complex that catalyzes the

\*To whom correspondence should be addressed (nicholas.reiter@marquette.edu).  
ORCID: Nicholas J Reiter: 0000-0002-6095-6528

**Conflict of Interest:** The authors declare that they have no conflict of interest.

conversion of precursor tRNA (ptRNA) into functional tRNA, facilitating the removal of the 5' leader RNA sequence (Guerrier-Takada et al. 1983). The RNA-based form of Ribonuclease P is a multi-turnover ribozyme found in almost all organisms yet relies on one or more protein subunits for increased catalytic efficiency and enzymatic function *in vivo*. Structural and biochemical studies of the RNase P have proven to be fundamental to our understanding of catalytic RNA structure and function, as well as RNA-based gene regulatory processes (see reviews: (Kazantsev and Pace 2006; Hartmann et al. 2009; Liu and Altman 2010; Mondragon 2013; Klemm et al. 2016)). However, the mechanism of action for this essential ribozyme and the multifunction roles of RNase P protein components, in bacteria and higher organisms, remain unresolved and incomplete (Klemm et al. 2016; Lemieux et al. 2016; Gopalan et al. 2017; Martin and Reiter 2017). Specifically, elucidating the conformational transitions that give rise to the formation of the RNA-based active site and defining the molecular details of how the RNase P protein components orient diverse RNA substrates will be required to better understand how dynamic RNP assemblies function as enzymes. The RNA-based form of RNase P serves as an ideal system to gain insight into the origins of RNA catalysis and to better understand the evolution of RNP complexes.

In bacteria, the RNase P holoenzyme is composed of a large RNA (~400 nucleotides), a small protein subunit (~120 amino acids), and at least two catalytically important metal ions. Crystallographic studies of the bacterial RNase P RNA alone and as a holoenzyme-product complex show how the active site is globally organized and how shape-dependent recognition occurs for the ptRNA substrate (Krasilnikov et al. 2003; Krasilnikov et al. 2004; Kazantsev et al. 2005; Torres-Larios et al. 2005; Reiter et al. 2010). In addition, biochemical studies show that the protein component can increase the enzyme's functionality and alter substrate recognition properties to facilitate RNase P activation (Crary et al. 1998; Kurz et al. 1998; Niranjankumari et al. 1998; Buck et al. 2005a; Buck et al. 2005b; Lin et al. 2016; Niland et al. 2016; Liu et al. 2017; Niland et al. 2017). At the molecular level, the P protein associates with three universally conserved regions of the catalytic RNA via basic amino acids and a bacterially conserved electropositive-rich  $\alpha$ -helix (Stams et al. 1998; Buck et al. 2005a; Reiter et al. 2010). Along with this key RNA-protein interaction, the formation of the RNP complex enables protein-mediated conformational transitions that help to optimally position, align, and discriminate RNA substrates adjacent to the enzyme active site (Crary et al. 1998; Buck et al. 2005a; Buck et al. 2005b; Christian et al. 2006; Sun et al. 2006; Hsieh and Fierke 2009; Koutmou et al. 2010; Sun et al. 2010; Reiter et al. 2012; Guenther et al. 2013). Thus, although RNase P function likely varies from different organisms, protein stabilization of the highly conserved P RNA sub-domain structure and protein recognition of the 5' ptRNA leader serve as key general properties of the RNase P holoenzyme.

The hyperthermophilic *Thermatoga maritima* RNase P undergoes reversible folding and has optimal activity at 50 °C (Paul et al. 2001; Buck et al. 2005a; Buck et al. 2005b). The *T. maritima* RNase P holoenzyme serves as excellent system to probe the dynamics of protein-ptRNA binding. Both the RNA and protein components of *T. maritima* RNase P are highly structured and both represent ideal biomolecules to examine how large RNA-protein complexes are assembled and become functional enzymes. Here, we report the  $^1\text{H}$ ,  $^{13}\text{C}$ , and  $^{15}\text{N}$  resonance assignments of the *T. maritima* RNase P protein. This study will help to illuminate the conformational transitions of a bacterial RNase P protein in the reaction

mechanism, from substrate recognition to facilitating the stabilization of the active site. Complete resonance assignments of the backbone and side chain residues will allow us to probe the dynamics of protein-ptRNA binding and define the motional properties associated with bacterial RNase P holoenzyme activation.

## Methods and experiments

### Sample preparation

The protein sample was prepared using the BL21 Gold *Escherichia coli* strain and derived from a pGEX4Ta vector that contained the *rnpA* gene from *T. maritima* and an N-terminal glutathione S-transferase (GST) fusion protein. The optimized expression protocol utilized M9 minimal media containing  $^{15}\text{NH}_4\text{Cl}$  and  $^{13}\text{C}_6\text{-D-glucose}$  (Cambridge Isotope Laboratories). A 3 mL starter cell culture was grown at 310 K (225 rpm) with 150ug/mL ampicillin for 20 hours and was used to inoculate 50 mL M9 media (200 ug/mL ampicillin). This 50 mL culture was grown at 310 K (225 rpm) for 12–14 hours and subsequently transferred into 2 L M9 media for 8–10 hours. When  $\text{OD}_{600}$  reached 1.0–1.2, temperature was reduced to 303 K and 1 mM isopropyl- $\beta$ -D-thiogalactopyranoside (IPTG) was added to induce expression 10–14 hours. Cells were subsequently harvested by centrifugation at 5000 g for 15 min, flash cooled in liquid nitrogen, and stored at  $-80^\circ\text{C}$  until use.

$^{15}\text{N}$ ,  $^{13}\text{C}$ -labeled RNase P protein purification followed the previous protocol (Krivenko et al. 2002) with the following modifications. Pellets were thawed on ice and fully resuspended in an appropriate volume of lysis buffer (50 mM Tris-HCl pH 7.5, 4 mM EDTA, 5% (v/v) glycerol, 0.1% (v/v) NP-40 and cOmplete™ protease inhibitor cocktail (Roche)). The cell suspension was lysed on ice by sonication for 13 cycles of 60 second bursts followed by 1 min pauses to prevent overheating. The lysate was separated by centrifugation at 28,000 g and 4 °C for 30 min. and the filtered lysate was treated with 800 NIH units of thrombin per 40 mL for overnight at room temperature. In this step, the GST was cleaved from the RNase P protein, resulting in a Gly-Ser sequence at the N-terminus.

The digested  $^{15}\text{N}$ ,  $^{13}\text{C}$ -labeled sample was purified following a protein denaturation - renaturation strategy that was previously developed (Paul et al. 2001; Buck et al. 2005a; Buck et al. 2005b). To denature the protein, lysate dilution buffer (50 mM Tris-HCl pH7.5, 4 mM EDTA, 8 M urea) was added into the sample to make a final concentration to 5 M urea. Sample was loaded on to a pre-equilibrated 15S cation exchange column (50 mM Tris-HCl pH 7.5, 0.2 mM EDTA, 5 M urea) and subsequently eluted with a linear gradient (50 mM Tris-HCl pH 7.5, 0.2 mM EDTA, 5 M urea, 2 M NaCl). Appropriate fractions containing the denatured  $^{15}\text{N}$ ,  $^{13}\text{C}$ -labeled RNase P protein were dialyzed against 4 L buffer of 50 mM Tris-HCl pH 7.5, 0.2 mM EDTA, 1 M NaCl for 1–2 days. After the protein was renatured, the sample solution was diluted to approximately 200mM NaCl and a second 15S cation exchange chromatography step was applied in the absence of urea, with a pre-equilibration buffer (50mM Tris-HCl pH7.5, 0.2mM EDTA) and an elution gradient containing 50mM Tris-HCl pH7.5, 0.2mM EDTA, and 3M NaCl. Highly pure  $^{15}\text{N}$ ,  $^{13}\text{C}$ -labeled RNase P protein fractions were pooled, concentrated, and extensively dialyzed against 2 L buffer (50 mM Tris-HCl pH 7.5, 0.2 mM EDTA). A final dialysis against 4 liters of 20 mM sodium

phosphate pH 6.0, 80 mM NaCl, 8 mM sodium sulfate solution was performed prior to NMR sample preparation. Protein purity was verified by SDS-PAGE.

### NMR spectroscopy

All NMR experiments were conducted using 400  $\mu\text{M}$   $^{15}\text{N}$ ,  $^{13}\text{C}$ -RNase P protein in 20 mM sodium phosphate pH 6.0, 80 mM NaCl, 50  $\mu\text{M}$  4, 4-dimethyl-4-silapentane-sulfonate (DSS) at 318 K with 5 % (v/v)  $\text{D}_2\text{O}$  in a 3 mm Norell® select series NMR tube unless noted. NMR spectra were acquired on Bruker Avance-III 600MHz, 800MHz and 900 MHz spectrometers, equipped with cryogenic probes, as well as Varian VNMRS 600 and 800 MHz spectrometer equipped with a cryogenic probe. For backbone assignments, ( $^1\text{H}$ ,  $^{15}\text{N}$ ) heteronuclear single quantum coherence (HSQC) and a set of traditional triple-resonance experiments were performed, including HNC0, HNCA, HN(CO)CA, HNCACB, CBCA(CO)NH, HN(CA)CO. Side-chain assignments were carried out using three-dimensional (H)C(CCO)NH, H(CCCO)NH, (H)CCH-TOCSY, H(C)CH-TOCSY,  $^{15}\text{N}$ -NOESY-HSQC,  $^{13}\text{C}$ -NOESY-HSQC and ( $^1\text{H}$ ,  $^{13}\text{C}$ ) HSQC for aliphatic and aromatic groups, respectively. The  $^{13}\text{C}$ -NOESY-HSQC and aliphatic and aromatic optimized 2D  $^{13}\text{C}$  HSQC experiments were obtained in 95% (v/v)  $\text{D}_2\text{O}$ .  $^1\text{H}$  chemical shifts were referenced with respect to internal DSS, and  $^{13}\text{C}$  and  $^{15}\text{N}$  chemical shifts were referenced indirectly using nuclei-specific gyromagnetic ratios (Wishart et al. 1995). Spectra were processed with Topspin 3.5.7 (Bruker Inc.) and NMRPipe (Delaglio et al. 1995), and analyzed by using CARA (Keller 2004) and Sparky (Goddard and Kneller).

### Assignments and data deposition

Excluding the N-terminal non-native glycine and serine, 110 of 114 non-proline residues were assigned in the ( $^1\text{H}$ ,  $^{15}\text{N}$ ) HSQC spectrum, which corresponds to 96.5% of the backbone amides (Figure 1). The amide groups of T2, L13, R14 and K90 remain unassigned due to peak overlap, solvent exchange, or intermediate exchange broadening on the millisecond timescale. 99.1% of both  $\text{C}^\alpha$  and  $\text{C}^\beta$  resonances were assigned, while backbone  $\text{C}'$  were 97.4% assigned. In addition, the side-chain assignments of  $\text{C}^\gamma$ ,  $\text{C}^\delta$  and  $\text{C}^\epsilon$  resonances, respectively, are 78.5%, 77.8% and 57.1% complete. Regarding the completeness of protons, 99.2% of  $\text{H}^\alpha$ , 99.0% of  $\text{H}^\beta$ , along with 91.8%, 84.8% and 50.6% of  $\text{H}^\gamma$ ,  $\text{H}^\delta$  and  $\text{H}^\epsilon$  resonances, respectively, were unambiguously assigned.

Among the side-chain residues, L13, R44, R89 and K51 contain three or more unassigned side-chain aliphatic resonances that were not observable or were potentially in the overlapped areas in spectra. In total, 741  $^1\text{H}$ , 547  $^{13}\text{C}$  and 115  $^{15}\text{N}$  chemical shifts are assigned for the 14.2 kDa protein. The  $^{13}\text{C}$  and  $^{15}\text{N}$  chemical shifts were internally referenced using 4,4-dimethyl-4-silapentane-1-sulfonic acid (DSS), according to the literature (Markley et al. 1998). The chemical shift data has been deposited at the Biological Magnetic Resonance Data Bank (BMRB) with the accession number 27307.

The secondary structure of *T. maritima* RNase P protein in solution was predicted by uploading the  $\text{H}^\text{N}$ , N,  $\text{C}^\alpha$ ,  $\text{H}^\alpha$ ,  $\text{C}^\beta$ ,  $\text{C}'$ , H chemical shifts to the TALOS-N webserver (Shen and Bax 2013). The comparison between the secondary structure from the prediction and the secondary structure of the crystal structure (PDB: 1NZ0) is illustrated in Figure 2. These

data show a high consistency, which indicate that the solution conformation of the protein at 0.4 mM is similar to the 1NZ0 structure. This result provides strong confidence in the resonance assignments of the *T. maritima* RNase P protein and will enable a comprehensive analysis of the motional properties associated with protein-ptRNA binding interface.

## Acknowledgments

This work was supported in part by grants for NMR instrumentation from the NSF (0922862), NIH (S10 RR025677) and Vanderbilt University. BPB acknowledges support from the NIGMS (T32GM007347). NJR acknowledges support from Vanderbilt University and Marquette University, as well as funding from the American Heart Association (14GRNT20380334) and the NIH (GM120572). The content is solely the responsibility of the authors and does not necessarily represent the official views of the National Institutes of Health.

## References

- Buck AH, Dalby AB, Poole AW, Kazantsev AV, Pace NR. a Protein activation of a ribozyme: the role of bacterial RNase P protein. *EMBO J.* 2005; 24:3360–3368. [PubMed: 16163391]
- Buck AH, Kazantsev AV, Dalby AB, Pace NR. Structural perspective on the activation of RNase P RNA by protein. *Nat Struct Mol Biol.* 2005b
- Christian EL, Smith KM, Perera N, Harris ME. The P4 metal binding site in RNase P RNA affects active site metal affinity through substrate positioning. *RNA.* 2006; 12:1463–1467. [PubMed: 16822954]
- Crary SM, Niranjanakumari S, Fierke CA. The protein component of *Bacillus subtilis* ribonuclease P increases catalytic efficiency by enhancing interactions with the 5' leader sequence of pre-tRNA<sup>Asp</sup>. *Biochemistry.* 1998; 37:9409–9416. [PubMed: 9649323]
- Delaglio F, Grzesiek S, Vuister GW, Zhu G, Pfeifer J, Bax A. NMRPipe: a multidimensional spectral processing system based on UNIX pipes. *Journal of Biomolecular NMR.* 1995; 6:277–293. [PubMed: 8520220]
- Goddard, TD., Kneller, DG. SPARKY 3. University of California; San Francisco: Available from: <https://http://www.cgl.ucsf.edu/home/sparky/>
- Gopalan V, Jarrous N, Krasilnikov AS. Chance and necessity in the evolution of RNase P. *RNA.* 2017 Sep 29. pii: rna.063107.117. doi: 10.1261/rna.063107.117
- Guenther UP, Yandek LE, Niland CN, Campbell FE, Anderson D, Anderson VE, Harris ME, Jankowsky E. Hidden specificity in an apparently nonspecific RNA-binding protein. *Nature.* 2013; 502:385–388. [PubMed: 24056935]
- Guerrier-Takada C, Gardiner K, Marsh T, Pace N, Altman S. The RNA moiety of ribonuclease P is the catalytic subunit of the enzyme. *Cell.* 1983; 35:849–857. [PubMed: 6197186]
- Hartmann RK, Gossringer M, Spath B, Fischer S, Marchfelder A. The making of tRNAs and more - RNase P and tRNase Z. *Progress in molecular biology and translational science.* 2009; 85:319–368. [PubMed: 19215776]
- Hsieh J, Fierke CA. Conformational change in the *Bacillus subtilis* RNase P holoenzyme--pre-tRNA complex enhances substrate affinity and limits cleavage rate. *RNA.* 2009; 15:1565–1577. [PubMed: 19549719]
- Kazantsev AV, Krivenko AA, Harrington DJ, Holbrook SR, Adams PD, Pace NR. Crystal structure of a bacterial ribonuclease P RNA. *Proc Natl Acad Sci U S A.* 2005; 102:13392–13397. [PubMed: 16157868]
- Kazantsev AV, Pace NR. Bacterial RNase P: a new view of an ancient enzyme. *Nat Rev Microbiol.* 2006; 4:729–740. [PubMed: 16980936]
- Keller, RLJ. The Computer Aided Resonance Assignment Tutorial. Cantina verlag: The Swiss Federal Institute of Technology Zürich, Switzerland; 2004.
- Klemm BP, Wu N, Chen Y, Liu X, Kaitany KJ, Howard MJ, Fierke CA. The Diversity of Ribonuclease P: Protein and RNA Catalysts with Analogous Biological Functions. *Biomolecules.* 2016;6. [PubMed: 26751493]

- Koutmou KS, Zahler NH, Kurz JC, Campbell FE, Harris ME, Fierke CA. Protein-precursor tRNA contact leads to sequence-specific recognition of 5' leaders by bacterial ribonuclease P. *Journal of Molecular Biology*. 2010; 396:195–208. [PubMed: 19932118]
- Krasilnikov AS, Xiao Y, Pan T, Mondragon A. Basis for structural diversity in homologous RNAs. *Science*. 2004; 306:104–107. [PubMed: 15459389]
- Krasilnikov AS, Yang X, Pan T, Mondragón A. Crystal structure of the specificity domain of ribonuclease P. *Nature*. 2003; 421:760–764. [PubMed: 12610630]
- Krivenko AA, Kazantsev AV, Adamidi C, Harrington DJ, Pace NR. Expression, purification, crystallization and preliminary diffraction analysis of RNase P protein from *Thermotoga maritima*. *Acta crystallographica Section D, Biological crystallography*. 2002; 58:1234–1236. [PubMed: 12077454]
- Kurz JC, Niranjanakumari S, Fierke CA. Protein component of *Bacillus subtilis* RNase P specifically enhances the affinity for precursor-tRNA<sub>Asp</sub>. *Biochemistry*. 1998; 37:2393–2400. [PubMed: 9485387]
- Lemieux B, Laterreur N, Perederina A, Noel JF, Dubois ML, Krasilnikov AS, Wellinger RJ. Active Yeast Telomerase Shares Subunits with Ribonucleoproteins RNase P and RNase MRP. *Cell*. 2016; 165:1171–1181. [PubMed: 27156450]
- Lin HC, Zhao J, Niland CN, Tran B, Jankowsky E, Harris ME. Analysis of the RNA Binding Specificity Landscape of C5 Protein Reveals Structure and Sequence Preferences that Direct RNase P Specificity. *Cell Chemical Biology*. 2016; 23:1271–1281. [PubMed: 27693057]
- Liu, F., Altman, S. Ribonuclease P. Springer Science+Business Media, LLC; New York: 2010.
- Liu X, Chen Y, Fierke CA. 2017 Inner-sphere Coordination of Divalent Metal Ion with Nucleobase in Catalytic RNA. *Journal of the American Chemical Society*. Nov 8. doi: 10.1021/jacs.7b08755
- Markley JL, Bax A, Arata Y, Hilbers CW, Kaptein R, Sykes BD, Wright PE, Wuthrich K. Recommendations for the presentation of NMR structures of proteins and nucleic acids. IUPAC-IUBMB-IUPAB Inter-Union Task Group on the Standardization of Data Bases of Protein and Nucleic Acid Structures Determined by NMR Spectroscopy. *Journal of Biomolecular NMR*. 1998; 12:1–23. [PubMed: 9729785]
- Martin WJ, Reiter NJ. Structural Roles of Noncoding RNAs in the Heart of Enzymatic Complexes. *Biochemistry*. 2017; 56:3–13. [PubMed: 27935277]
- Mondragon A. Structural studies of RNase P. *Annual Review of Biophysics*. 2013; 42:537–557.
- Niland CN, Anderson DR, Jankowsky E, Harris ME. The contribution of the C5 protein subunit of *Escherichia coli* ribonuclease P to specificity for precursor tRNA is modulated by proximal 5' leader sequences. *RNA*. 2017; 23:1502–1511. [PubMed: 28694328]
- Niland CN, Zhao J, Lin HC, Anderson DR, Jankowsky E, Harris ME. Determination of the Specificity Landscape for Ribonuclease P Processing of Precursor tRNA 5' Leader Sequences. *ACS Chemical Biology*. 2016; 11:2285–2292. [PubMed: 27336323]
- Niranjanakumari S, Stams T, Crary SM, Christianson DW, Fierke CA. Protein component of the ribozyme ribonuclease P alters substrate recognition by directly contacting precursor tRNA. *Proc Natl Acad Sci USA*. 1998; 95:15212–15217. [PubMed: 9860948]
- Paul R, Lazarev D, Altman S. Characterization of RNase P from *Thermotoga maritima*. *Nucleic Acids Research*. 2001; 29:880–885. [PubMed: 11160919]
- Reiter NJ, Osterman A, Torres-Larios A, Swinger KK, Pan T, Mondragon A. Structure of a bacterial ribonuclease P holoenzyme in complex with tRNA. *Nature*. 2010; 468:784–789. [PubMed: 21076397]
- Reiter NJ, Osterman AK, Mondragon A. The bacterial ribonuclease P holoenzyme requires specific, conserved residues for efficient catalysis and substrate positioning. *Nucleic Acids Research*. 2012
- Shen Y, Bax A. Protein backbone and sidechain torsion angles predicted from NMR chemical shifts using artificial neural networks. *Journal of Biomolecular NMR*. 2013; 56:227–241. [PubMed: 23728592]
- Stams T, Niranjanakumari S, Fierke CA, Christianson DW. Ribonuclease P protein structure: evolutionary origins in the translational apparatus. *Science*. 1998; 280:752–755. [PubMed: 9563955]

- Sun L, Campbell FE, Yandek LE, Harris ME. Binding of C5 Protein to P RNA Enhances the Rate Constant for Catalysis for P RNA Processing of Pre-tRNAs Lacking a Consensus G(+1)/C(+72) Pair. *Journal of Molecular Biology*. 2010; 395:1019–1037. [PubMed: 19917291]
- Sun L, Campbell FE, Zahler NH, Harris ME. Evidence that substrate-specific effects of C5 protein lead to uniformity in binding and catalysis by RNase P. *The EMBO journal*. 2006; 25:3998–4007. [PubMed: 16932744]
- Torres-Larios A, Swinger KK, Krasilnikov AS, Pan T, Mondragon A. Crystal structure of the RNA component of bacterial ribonuclease P. *Nature*. 2005; 437:584–587. [PubMed: 16113684]
- Wishart DS, Bigam CG, Yao J, Abildgaard F, Dyson HJ, Oldfield E, Markley JL, Sykes BD. 1H, 13C and 15N chemical shift referencing in biomolecular NMR. *Journal of Biomolecular NMR*. 1995; 6:135–140. [PubMed: 8589602]

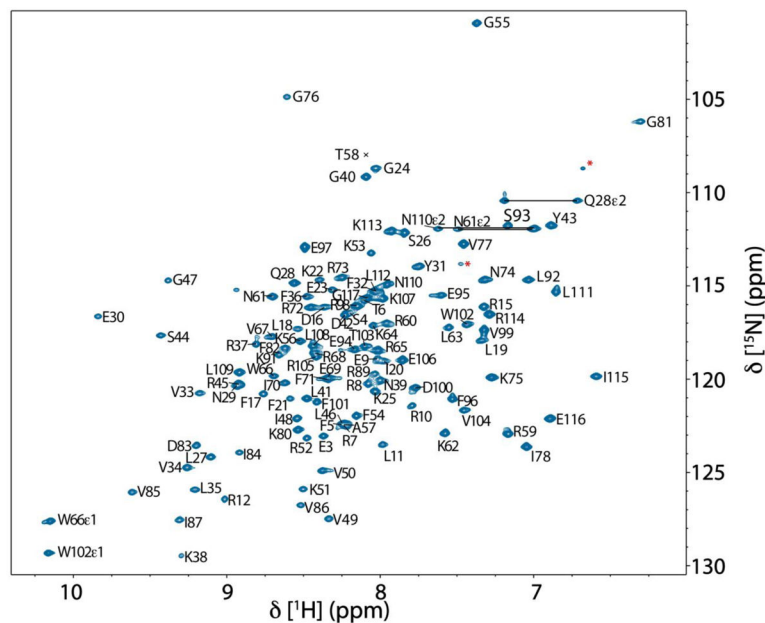


**Fig. 1.** 900 MHz ( $^1\text{H}$ ,  $^{15}\text{N}$ ) HSQC spectrum of 400  $\mu\text{M}$  *T. maritima* RNase P protein in 20 mM sodium phosphate (pH 6.0), 80 mM NaCl, 50  $\mu\text{M}$  DSS, 8 mM sodium sulfate, and 5 %  $\text{D}_2\text{O}$  at 318 K. Assigned residues are indicated using *single letter codes*. Side-chain  $\text{NH}_2$  resonances of asparagine and glutamine are connected by *horizontal lines*. Signals labeled by *red asterisks* likely derive from arginine  $\epsilon\text{NH}$  resonances while those non-labeled are likely from minor population of the structural conformations in the sample. The assigned resonances with only a *black cross* indicate the position of the residue below the spectrum's intensity levels. *Numbering of T. maritima* RNase P protein corresponds to the gene sequence RNPA\_THEMA (UniProtKB - Q9X1H4).



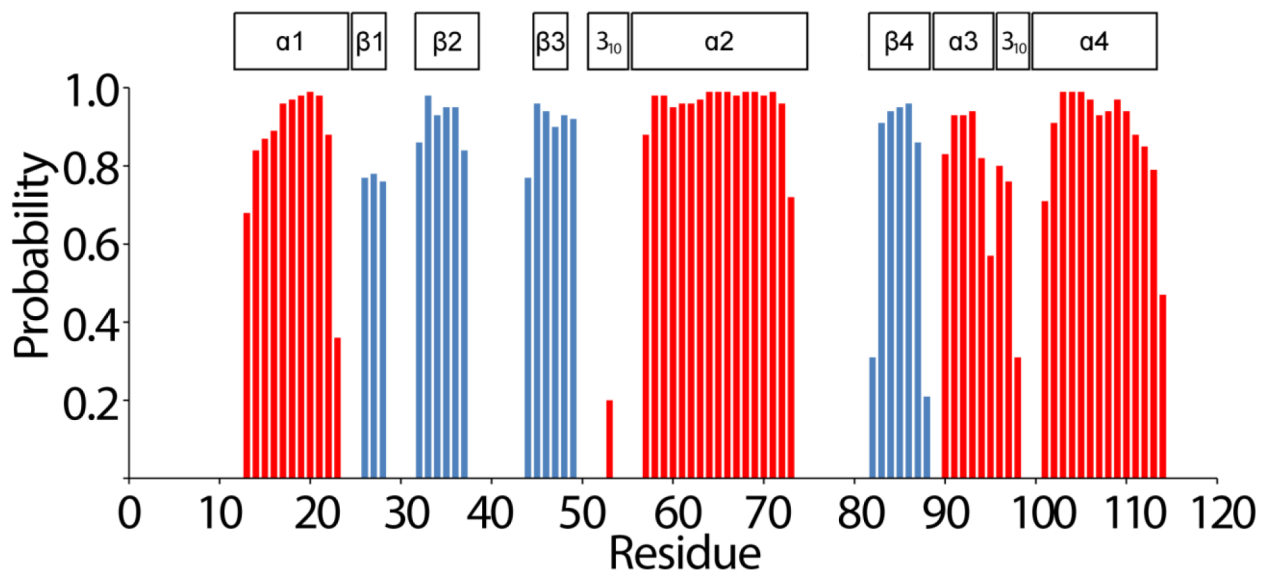


**Fig. 2.** TALOS-N prediction of secondary structure elements of *T. maritima* RNase P protein derived from  $H^N$ , N,  $H^\alpha$ ,  $C^\alpha$ ,  $C^\beta$  and  $C'$  chemical shifts. The secondary structure probability is reflected by the *height of the bars* (blue  $\beta$ -strand, red  $\alpha$ -helices). For comparison, the positions of secondary structure elements according to the crystal structure (PDB entry 1ZN0) are indicated *above* the amino acid residues.